Electronic Supporting Material

Ultrafast nonequilibrium dynamic process of separate electron and hole during exciton formation in few-layer tungsten disulfide

Junjie Chen[1,†], Sen Guo[1,†], Dabin Lin[1], Zhaogang Nie[1,*], Chung-Che Huang[2], Cheng Wang[1], Kaige Hu[1], Fangteng Zhang[1], Weiren Zhao[1], Wenchun Zhang[3]

[1] School of Physics and Optoelectronic Engineering, Guangdong University of Technology, Guangzhou 510006, Guangdong, China

[2] Optoelectronics Research Centre, University of Southampton, Southampton SO17 1BJ, United Kingdom

[3] College of Traditional Chinese Medicine, Jiangxi University of Traditional Chinese Medicine, Nanchang 33004, China

† These authors contributed equally.

* Address correspondence to zgnie@gdut.edu.cn

1. Optical characterizations of the sample and laser spectra

Fig. S1(a) shows the steady-state absorption spectrum of four-layer WS_2. To distinguish the contributions of exciton transitions and the tail of the CB to the measured steady-state absorption [S1,S2], the spectrum is fitted to a three-Gaussian function superimposed on a cubic polynomial. The components of the converged fit are shown in Fig. S1(b) and (c), respectively. The narrowband pump laser spectra for resonant excitation of X_A absorption band are shown together in Fig. S1(d). The pump spectra at 625 nm and 655 nm are respectively on the blue and red sides of X_A resonance band. The narrowband pump pulse resonantly excites the X_A transition, promoting electrons from K_{v1} to K_c, following which the differential absorption of a broadband probe pulse that spans X_A and X_B transitions (see Fig. 1(a)). Fig. S1(e) exhibits the Raman spectrum of the four-layer WS_2. As shown, the E^1_{2g} and A_{1g} modes are respectively located at 356.4 and 420.3 cm^{-1}, where the frequency difference between the two modes is about 63.9 cm^{-1}. The difference corresponds to the thickness of four-layer WS_2 [S3]. The Raman spectra were collected at several points to check the sample quality. Except some very tiny dusts on the surface, the sample is quite uniform. A part of the optical image of the sample is shown in the

inset of Fig. S1(e), which shows the sample is a big-size uniform membrane.

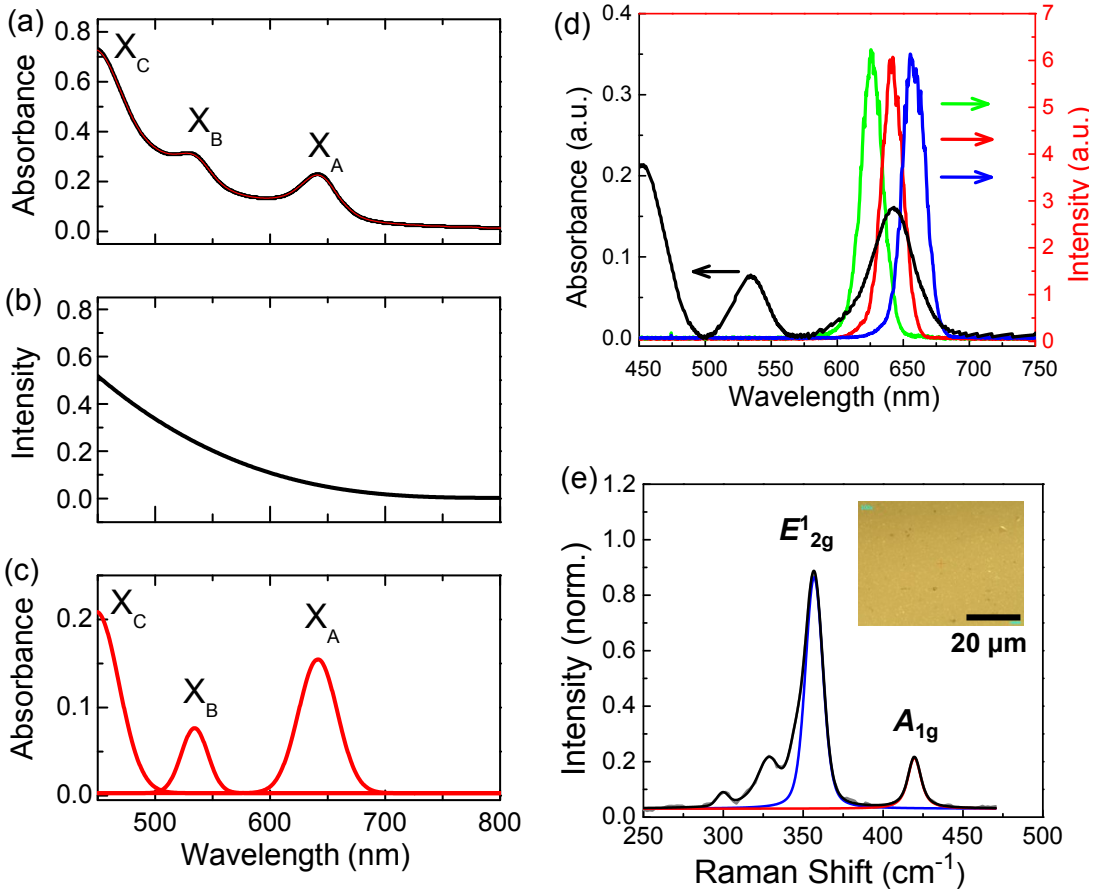

Fig. S1 (a) Steady-state absorption spectrum of the four-layer WS_2 on a fused silica substrate collected at 300 K. The solid red line is a three-Gaussian superimposed on a cubic polynomical function. (b) The cubic polynomical component and (c) the three Gaussian curves for the fitting. (d) The narrowband pump laser spectra peaking at 625 nm (green line), 640 nm (red line) and 650 nm (blue line) for resonant X_A excitations. The stationary absorption spectrum after removing the cubic polynomical component (black line) is shown together with the narrowband pump laser spectra. (e) Raman spectrum (Gray line) of the four-layer WS_2 on fused silica substrates. The spectrum is fitted by multiple GaussAmp peak functions. The black line is the cumulative fitting line. For clarity, we retain only the two fitting peaks of E^1_{2g} (blue line) and A^1_g (red line). The inset is a part of the optical image of the sample, which shows the sample is a big-size uniform membrane.

2. Cross-correlation trace

The time resolution of the experimental apparatus is measured by performing a second-order pump-probe intensity cross-correlation with a type I beta barium borate (BBO) crystal located at the sample position, which allows the determination of zero

time delay to <2 fs accuracy. The resultant cross-correlation trace between the broadband probe pulse and the pump pulse peaking at 640 nm yields a time resolution of 65 fs fwhm for the apparatus, as shown in Fig. S2(a). In addition, to characterize the pulse duration of the broadband pulse at the sample position, the autocorrelation trace between the broadband pump and probe pulses with a sample laser spectrum was also collected, as plotted in Fig. S2(b), which indicates a fwhm of 13.6 fs, corresponding to a laser pulse duration of 9.6 fs.

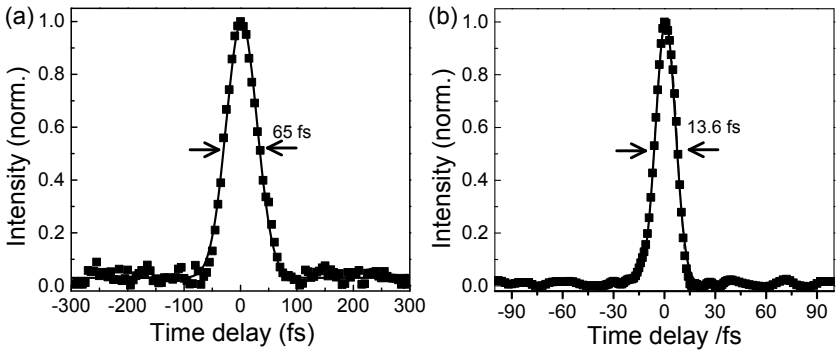

Fig. S2 Intensity cross-correlation traces of pump and probe pulses, revealing a time resolution of 65 fs fwhm for the apparatus.

3. Pump fluence-dependence measurements

A log-log plot of the peak ΔA signal *S* obtained at the X_A transition as a function of fluence *F* is shown in Fig. S3. Since *S* is proportional to the F^N, the slope of the log-log plot yields the photon order N, which is 1.03 ± 0.04. This result confirms that the excitation in our experiments occurs in the linear regime.

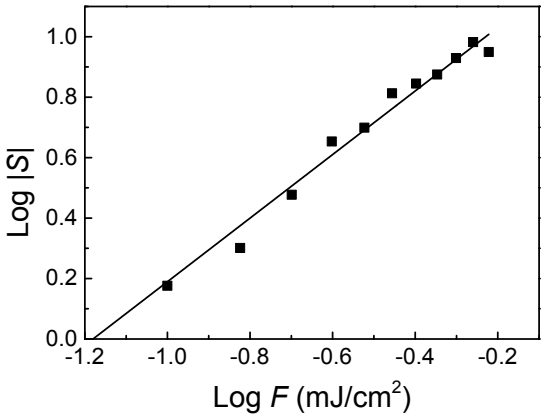

Fig. S3 Dependence of the maximum ΔA signal *S* on the pump fluence *F*, confirming one photon excitation of the sample. |*S*| is the absolute value of the signal *S*.

4. ΔA spectra obtained by pumping at 655 nm

Fig. S4(a) presents the 2D plot of ΔA spectra obtained by resonant excitation on the red side of the X_A resonance band at 655 nm, where the colour scale, the horizontal axis and the vertical axis represent the magnitude of ΔA, the probe wavelength and the pump–probe time delay, respectively. The dotted contour lines indicate that the initial part in the early time range of X_A resonance is distorted to the direction of lower energy, while the X_B resonance is not. This can be further evidenced from $\langle M_{e+h}^{(1)}(t)\rangle$ (red solid line) and $\langle M_e^{(1)}(t)\rangle$ (black solid line) traces in Fig. S4(a). The behavior of $\langle M_{e+h}^{(1)}(t)\rangle$ is quite similar to the phenomena pumped at 640 nm, exhibiting a similar red- and blue-shift crossover in the initial time range, and a sharp initial decay appears simutaneously in the peak traces due to X_A transition, as shown in Fig. S4(b). For the X_B transition, it is still similar to that under resonant 640 nm excitation, there isn't obvious initial shift in $\langle M_e^{(1)}(t)\rangle$ trace and also no obvious sharp decay appears in the peak trace due to X_B transition.

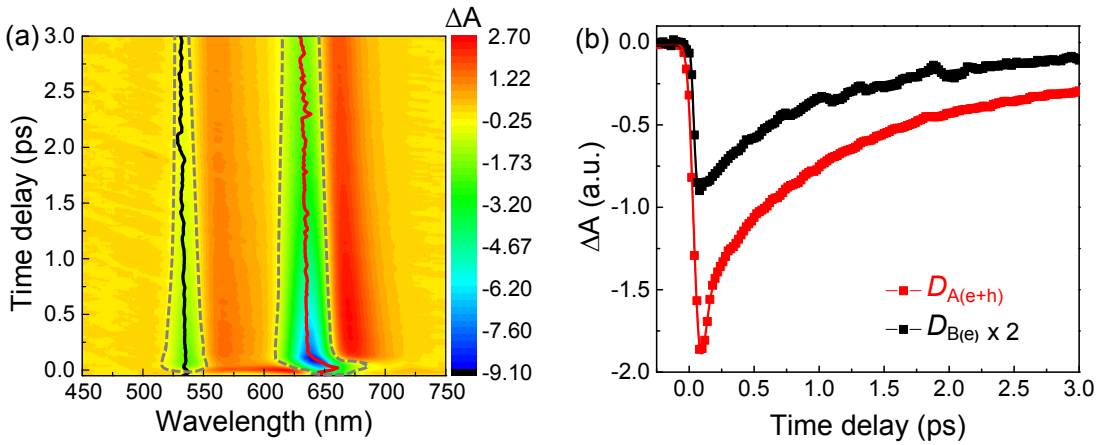

Fig. S4 (a) 2D plot of ΔA spectra obtained by a pump pulse peaking at 655 nm (See Fig. S1(d)). The sample temperature is 300 K, and the pump fluence is 0.32 mJ/cm^2. The solid red and black lines are the $\langle M_{e+h}^{(1)}(t)\rangle$ and $\langle M_e^{(1)}(t)\rangle$ traces respectively for X_A and X_B transitions. The dotted gray lines are the contour lines for eye guides to show the peak shift of X_A and X_B resonances. (b) $D_{A(e+h)}$ and $D_{B(e)}$ peak traces probed at 640 nm and 530 nm respectively for X_A and X_B transitions.

Reference

[S1] G. Wang, Chernikov, A. Glazov, M. M. Heinz, T. F. Marie, X. Amand, T. B. Urbaszek, *Rev. Mod. Phys.*, 2018, **90**, 021001.

[S2] H. Chen, X.Wen, J.Zhang, T. Wu, Y. Gong, X. Zhang, J. Yuan, C. Yi, J. Lou, P. M. Ajayan, W. Zhuang, G. Zhang, J. Zheng, *Nat. Commun.,* 2016, **7**, 12512.

[S3] Y. Li, X. Li, T. Yu, G. Yang, H. Chen, C. Zhang, Q. Feng, J. Ma, W. Liu, H. Xu, Y. Liu, and X. Liu, *Nanotechnology*, 2018, **29**, 124001-124009.